Temperature dependence of the lower critical field of high-T_c superconducting crystals near T_c

F. Mrowka, M. Wurlitzer, and P. Esquinazi
Department of Superconductivity and Magnetism, Universität Leipzig, Linnéstrasse 5, D-04103 Leipzig, Germany

E. Zeldov
Department of Condensed Matter Physics, The Weizmann Institute of Science, 76100 Rehovot, Israel

T. Tamegai and S. Ooi
Department of Applied Physics, The University of Tokyo, Hongo, Bunkyo-ku, Tokyo, 113, Japan

K. Rogacki* and B. Dabrowski
Department of Physics, Northern Illinois University, DeKalb, Illinois 60115
(Received 31 March 1998; revised manuscript received 22 March 1999)

We have measured the nonlinear susceptibility of $YBa_2Cu_4O_8$, $Bi_2Sr_2CaCu_2O_8$, and untwinned $YBa_2Cu_3O_7$ crystals near the superconducting critical temperature T_c in order to determine the lower critical field $H_{c1}(T)$. The ac field amplitude dependence of the susceptibility for homogeneous $YBa_2Cu_4O_8$ and $Bi_2Sr_2CaCu_2O_8$ crystals is in agreement with the geometrical barrier model allowing us to determine the penetration field $H_p(T) \propto H_{c1}(T)$. We clearly show that in these crystals the previously reported breakdown of H_{c1} near T_c coincides with the low-temperature ac field amplitude independent onset of the superconducting transition. We show that this anomalous behavior of $H_{c1}(T)$ is due to the influence of inhomogeneities and it is not an intrinsic property. We have also investigated the influence of the earth field on the nonlinear susceptibility, and we demonstrate the importance of its shielding for careful measurements of H_{c1} near T_c. [S0163-1829(99)10029-8]

I. INTRODUCTION

Previous investigations of the lower critical field $H_{c1}(T)$ of high-T_c superconductors (HTS's) showed an anomalous temperature dependence and, in some cases, a sudden suppression near the mean field superconducting critical temperature T_c.[1–7] For example, superconducting quantum interference device measurements of the zero-field-cooled flux expulsion and remanent moment measurements[2] as well as magnetic flux relaxation measurements[6] on several $YBa_2Cu_3O_7$ (Y123) crystals reported a collapse of $H_{c1}(T)$ at temperatures 1 to 2 K below T_c. A similar collapse of $H_{c1}(T)$, but at $\sim$3 K below T_c has been measured in $Bi_2Sr_2CaCu_2O_8$ (Bi2212) crystals using a micro-Hall probe.[5] Strikingly, micro-Hall probe measurements[5] did not find similar effects in Y123 crystals, in contradiction with the results reported in Refs. 2,6.

Several theoretical works and interpretations tried to clarify this breakdown of the Meissner state. It was speculated that the collapse of $H_{c1}(T<T_c)$ is due to the loss of phase coherence and decoupling of the stacks of superconducting CuO_2 planes.[2] Also, it has been suggested that the spontaneous production of thermally activated vortex-antivortex pairs at a Kosterlitz-Thouless-type transition[8] may cause H_{c1} to vanish below T_c. On the other hand, it has been argued that the spontaneous creation of vortex-antivortex pairs cannot occur in a quasi-two-dimensional system such as Bi2212.[9] Instead, fluctuations of the order parameter within the vortices would produce a downward renormalization of H_{c1} a few degrees below T_c.[9] This theory[9] predicts that the renormalization of $H_{c1}(T)$ depends strongly on the anisotropy of the crystal. The renormalization of $H_{c1}(T)$ due to fluctuations[9] predicts neither its collapse nor a negative curvature for Y123-based HTS, in apparent contradiction with the results of Refs. 2,6.

Apparently neither the experimental evidence nor the theoretical work has resulted in consent in this field, and more and clear experimental results are needed. Therefore, in this work we use the approach based on the measurement of the global susceptibility, as an attempt to measure the penetration field in HTS crystals with different anisotropies. Our results indicate an anomalous temperature dependence of $H_{c1}(T)$ near T_c for the Y124 and Bi2212 crystals, and its collapse at the low-temperature onset of the superconducting transition indicating that sample inhomogeneities cause this anomaly. The results of a Bi2212 crystal before and after annealing support this conclusion.

II. EXPERIMENTAL DETAILS

A. Sample characterization

The susceptibility signal of a weak pinning superconducting platelet at low applied fields (in our case $H \leqslant 10$ Oe) in perpendicular geometry depends mostly on vortex penetration through a barrier of geometrical origin.[10,11] Therefore, we were careful to choose appropriate crystals for our studies, based on the behavior of the nonlinear susceptibility. Three crystals, reported in this paper, are thin platelets with nearly rectangular shapes and smooth surfaces. Samples with rough surfaces, of irregular shapes or rounded rims proved to be inadequate for these investigations. Nevertheless and in order to get a better characterization of the influence of in-

TABLE I. Characteristics of the measured crystals. Bi2212a and Bi2212b are two $Bi_2Sr_2CaCu_2O_8$ crystals from different batches. The crystal Bi2212a# is the crystal Bi2212a after annealling 10 min at 900 °C and a rapid cooling thereafter. Y123 and Y124 denote the untwinned $YBa_2Cu_3O_7$ and the $YBa_2Cu_4O_8$ crystals. $2W$ is the total width and d the thickness of the crystal. The ratio between the lower critical field and the penetration field, H_{c1}/H_p, was calculated using Eq. (1).

Crystal	Size ($l\times w\times d$) [μm]	T_c [K]	$2W/d$	H_{c1}/H_p
Bi2212a	390×300×18	90.2	17	4.5
Bi2212a#	390×300×18	90.6	17	4.5
Bi2212b	1100×900×30	90.0	30	6
Y124	750×410×20	78.9	20	5
Y123	~2000×600×150	89.0	4	2.7

homogeneities in the measured properties, we have measured also an inhomogeneous Bi2212 crystal (Bi2212b).

Table I shows the critical temperature and the dimensions of the studied crystals. Magneto-optical measurements of the magnetic flux distribution in the Bi2212a crystal at 10 K and at 10 Oe applied dc field, show a symmetrical pattern, as published for other HTS's,[12] without indication of an anomalous penetration of flux due to shape or superconducting inhomogeneities. We note, however, that because these results are obtained at low temperatures cannot necessarily be extrapolated to T_c. This crystal was annealed 10 min at 900 °C in air and then rapidly cooled (Bi2212a). For the Bi2212b crystal a nonsymmetric, inhomogeneous flux distribution pattern was observed.

Figures 1 and 2 show the superconducting transition of three crystals measured by the real component of the ac susceptibility. The Y124 crystal was characterized in previously published studies.[11] The Y123 crystal showed no twinning planes under polarization microscope and, as the Y124 crystal, has no further annealing.

The critical temperature T_c is defined at the onset of the diamagnetic signal $\chi'(T)$, see Figs. 1 and 2 and below. This signal was measured with an ac field applied perpendicular to the main area, i.e., parallel to the c axis of the crystals, with the earth field compensated. The other component of the earth field parallel to the CuO_2 planes was not compensated. Most of the measurements of the ac susceptibility have been performed with an ac field frequency of 166 Hz, using sine-wave integration with respect to the fundamental frequency.

In Figs. 1 and 2 we see clearly that the width of the transition measured by the susceptibility depends on the amplitude of the applied ac field H_0. In general, a large ac field amplitude broadens the transition and shifts the onset of diamagnetism to lower temperatures. This broadening is related to the critical current density of the sample and the distribution of the shielding currents generated by the applied ac field. This broadening is not related necessarily to inhomogeneities.

A curious behavior of the transition and its ac field amplitude dependence is observed for the Bi2212a crystal, see Fig. 1. Its transition becomes narrower decreasing H_0, down to $\mu_0 H_0 \sim 200$ μT where it reaches a width of ~0.2 K. At

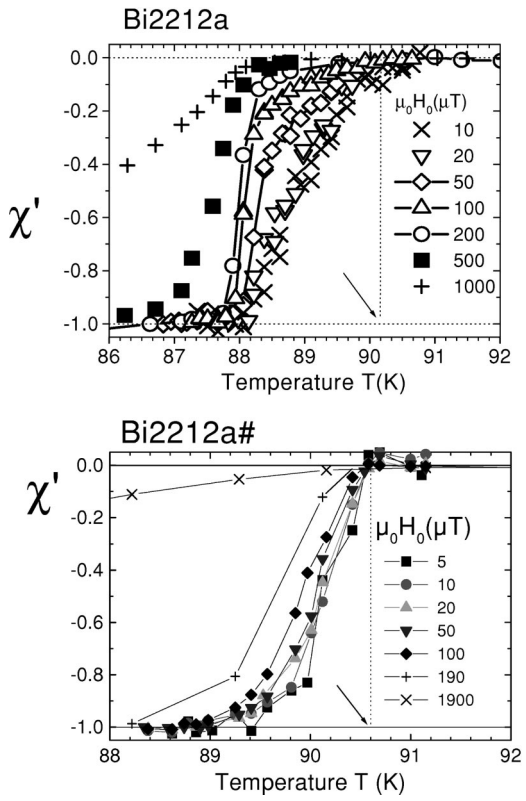

FIG. 1. Temperature dependence of the real component of the ac susceptibility measured at low ac field amplitudes H_0 and with the earth field compensated for the crystals Bi2212a and Bi2212a#. The arrows indicate the defined superconducting transition temperature T_c. The continuous and dotted lines are guides to the eye.

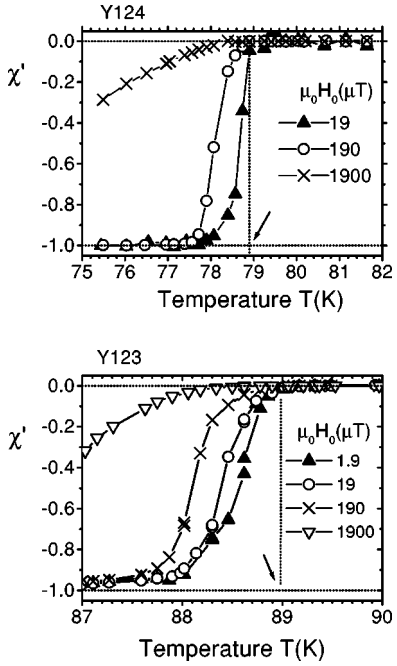

FIG. 2. Temperature dependence of the real component of the ac susceptibility measured at low ac field amplitudes H_0 and with the earth field compensated for the crystals Y124 and Y123. The arrows indicate the defined superconducting transition temperature T_c. The continuous and dotted lines are guides to the eye.

lower ac field amplitudes, however, the width of the transition increases and becomes independent of H_0 at $\mu_0 H_0 \leqslant 20$ μT, within the resolution of our measurements. At this low ac field amplitudes the transition width reaches a maximum value of ~ 2 K. As will become clear below, the observed behavior is due to the existence of a geometrical barrier and the influence of inhomogeneities on it. This barrier vanishes at $T \simeq 88$ K.

After annealing the Bi2212a crystal the ac response changed drastically. The transition width at similar ac field amplitudes is smaller. The apparent decrease of the transition width increasing the ac field amplitude as observed in the crystal before annealing, is not measured, see Fig. 1.

For the inhomogeneous crystal Bi2212b, we observed that for ac field amplitudes $\mu_0 H_0 \leqslant 200$ μT, the transition shows a shift in temperature, with a gradual decrease of its width in contrast to the behavior observed for the Bi2212a crystal shown in Fig. 2. Also, the susceptibility does not show perfect shielding at the low-temperature onset of the transition, but only at low enough temperatures. This behavior is also observed for a smaller crystal obtained by cutting the original Bi2212b crystal.

B. Experimental determination of the penetration field $H_p(T)$

The electromagnetic behavior of thin superconductors of various shapes has been subject of several experimental and theoretical studies, especially when the magnetic field is applied perpendicular to the main area of the platelet.[10–30] Theoretically[13–17,21] and experimentally[29] it has been shown that in transverse geometry the nonlinear response of a superconductor with relatively large pinning is not accounted for correctly by the Bean critical state model.[31] In our case, nonlinear response means the ac field dependence of the susceptibility at constant temperature and dc field.

The simple assumptions of the Bean model have to be modified in the transverse geometry due to demagnetization factors, that enhance the external field at the edges of the sample. We have recently showed that the ac field dependence of the ac susceptibility of structured Y123 thin films in transverse magnetic fields[29] can be well understood assuming bulk pinning and a generalized Bean model.[15,17,13,22]

For platelet samples with relatively low pinning, in sufficiently small dc fields and in transverse geometry, the nonlinear ac susceptibility near T_c can be well explained by the existence of a geometrical barrier, which originates from its flat shape.[10,11,23–25] This barrier prevents the penetration of flux into the sample at applied fields that are smaller than the characteristic penetration field H_p. If pinning can be neglected and the thickness is sufficiently constant over the whole area, a penetrating vortex undergoes only the influence of the Lorentz force caused by the Meissner currents flowing in the crystal and driving the vortex towards the center of the sample.[23,24] The corresponding vortex potential has a minimum in the center and a positive maximum at the edges. Flux lines can penetrate only from the rims into the sample, if they overcome this potential barrier, i.e., if the applied external field exceeds H_p. This penetration field has been derived[23,26] for a thin, narrow superconducting strip of rectangular shape of width $2W$ and thickness d, given by

$$H_p = \frac{2H_{c1}}{\pi} \operatorname{arctanh} \{\sqrt{1-[1-(d/2W)]^2}\}. \qquad (1)$$

For $d \ll 2W$ one can simplify Eq. (1) as $H_p \simeq (2H_{c1}/\pi)\sqrt{d/W}$, revealing that the demagnetization factor (in the present case $\sim\sqrt{d/W}$) is reduced as compared to that obtained for an elliptical shape $\sim d/W$.[23,19] For fields $H < H_p$ flux lines penetrate only into the narrow region near the rims of a width of the order $d/2$.[23,26] Recent numerical results for the thin-strip limit ($d \ll 2W$) give a slightly different relation for the penetration field[32]

$$H_p = 0.56 H_{c1}\left(\frac{d}{2W}\right)^{1/2}. \qquad (2)$$

We note that according to the geometrical barrier model the temperature dependence of $H_p(T)$ and $H_{c1}(T)$ are the same. Detailed calculations of the local flux density across the sample and of the static hysteresis,[10,23–25] as well as of the nonlinear susceptibilities χ' and χ'', were confirmed by dc and ac susceptibility measurements,[10,11,23,26,33] and also by scanning ESR probe measurements.[34] The geometrical barrier model predicts a discontinuity of the nonlinear ac susceptibility at the field amplitude $H_0 = H_p$, which can be explained as follows: (a) If the amplitude of the external field $H_0 < H_p$, the flux lines penetrate only in a narrow zone at the edges of the sample with a maximum width $\sim d/2$.[10] Therefore, the periodical variation of the external field gives an ac susceptibility that reflects the Meissner state, i.e., $\chi' \approx \chi'_{\text{Meissner}}$ and $\chi'' \approx 0$, independent of H_0. (b) If $H_0 > H_p$, the penetration of flux lines into the center of the sample leads to a hysteretic behavior with hysteresis losses (a finite χ'') and causes a breakdown of the (negative) χ' component. These predictions of the geometrical barrier model have been already demonstrated on suitable crystals[11] near $T_c (H \sim 0)$. Therefore, measuring the penetration field and the geometry of the sample one can determine H_{c1} near T_c using Eq. (1) or (2).

C. Influence of the earth field

Since our aim is to measure the lower critical field near T_c, we should be able to detect penetration fields of the order of 10μT or less. Therefore, the shielding of the earth magnetic field is necessary, at least in the direction perpendicular to the main surface of the crystals (parallel to the c axis).

With a small solenoid surrounding the primary and secondary coils used for the susceptibility measurements, we can apply a variable dc field H_{dc} normal to the sample surface. To measure and to shield the earth or any other dc field H_e at the sample position, we measure the second harmonic signal of the crystal as a function of the applied field H_{dc} at a constant temperature $T < T_c$. If the total dc field on the sample $H_t = H_{\text{dc}} + H_e > 0$ and the applied ac field amplitude $H_0 > H_p$, the second harmonic signal will be finite due to the asymmetry in the magnetization loop. By applying a dc field $H_{\text{dc}} = H_{\text{comp}}$ we can compensate H_e so that the total dc field at the sample becomes zero and the second harmonic signal vanishes. Therefore, we can determine $H_e = -H_{\text{comp}}$ at the sample. Using this procedure we have measured H_e at the

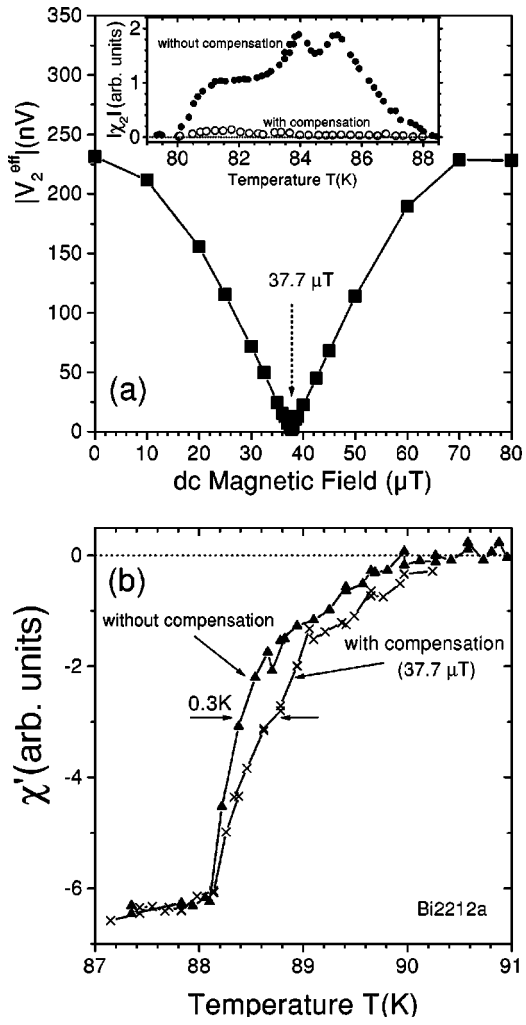

FIG. 3. (a) Second harmonic signal as a function of dc field. The signal vanishes at a dc field which compensates exactly the external (earth and surroundings) field on the sample. The measurements were done on the Bi2212a crystal at a temperature ~ 3 K below T_c. The inset shows the second harmonic signal as a function of temperature with and without compensation of the earth field. (b) Real part of the susceptibility of the same Bi2212 sample as a function of temperature with and without compensation of the earth field. The ac field amplitude used for this measurement was $\mu_0 H_0 = 25$ μT at a frequency of 166 Hz.

position of the Bi2212 crystal, see Fig. 3(a). From the measurements depicted in Fig. 3(a) we determine a field $\mu_0 H_e = 37.7$ μT, in good agreement with the field measured using a Hall probe outside the cryostat. In the inset of Fig. 3(a) we show the second harmonic signal as a function of temperature, with and without compensation, indicating that the extracted value of H_e does not depend on T, at least in the temperature range of our measurements.

Figure 3(b) shows the susceptibility of the Bi2212a crystal as a function of temperature, with and without earth field compensation. It is interesting to note that the compensation of the earth field shifts the transition to higher temperatures by $\simeq 0.3$ K. In the next section we will discuss the influence of the earth field on the ac field dependence of the susceptibility.

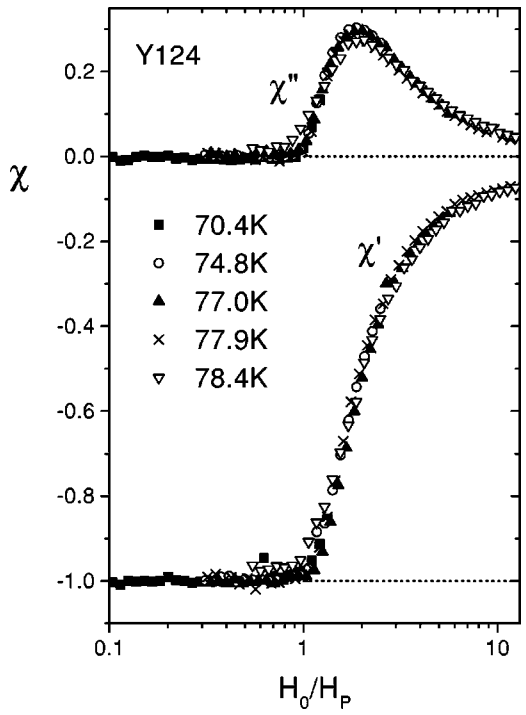

FIG. 4. The two components of the nonlinear ac susceptibility of the Y124 crystal at different temperatures (earth field compensated). The amplitude of the ac field H_0 is normalized by the penetration field H_p determined by the kink in the imaginary or real component of the susceptibility.

III. RESULTS

A. $YBa_2Cu_4O_8$

Figure 4 shows the two components of the nonlinear ac susceptibility for the Y124 crystal with earth field compensation. In the measured temperature range 70 K$<T<T_c$ the behavior of the nonlinear susceptibility can be well described by the geometrical barrier model, as shown already in Ref. 11. Note that when the ac field amplitude is normalized by H_p the results follow a single curve as predicted by theory. In the measured temperature range H_p varies by a factor of 50. The normalization of the two components is done dividing both signals by the value of the susceptibility in the Meissner state. The Meissner signal was measured with an ac field amplitude $H_0 = 1$ μT and at a temperature of 4.2 K.

At a temperature $T = 78.5$ K the penetration field $\mu_0 H_p \simeq 38$ μT is of the order of the measured vertical component of the earth field H_e. Therefore the geometrical barrier can be overcome by the earth field. The typical behavior of the nonlinear susceptibility observed at lower temperatures is lost when the earth field is not shielded, as demonstrated in Fig. 5. This measurement explains partially the loss of the geometrical barrier character of the curves measured in Ref. 11 near T_c. All the measurements of the ac field dependence of the susceptibility that are shown below have been done with the earth field vertical component compensated.

Figure 6 shows the temperature dependence of the penetration field $H_p(T)$; note that for this sample the lower critical field $H_{c1}(T) \simeq 5 H_p(T)$ using Eq. (1). It is clearly seen that H_p shows a negative curvature. The extrapolation indicates that it tends to vanish at $T_{co} \simeq T_c - 0.2$ K (see inset in

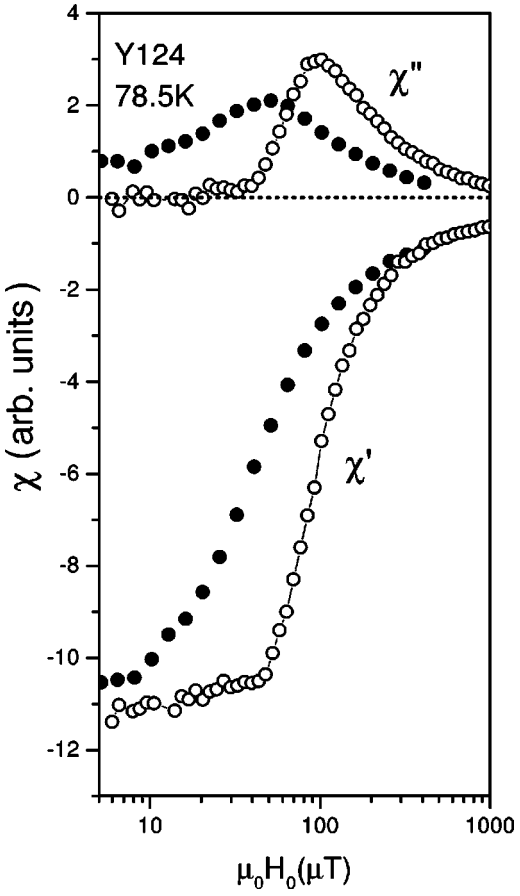

FIG. 5. The two components of the nonlinear ac susceptibility for the Y124 crystal at $T=78.5$ K. The two curves were obtained with (○) and without (●) compensation of the vertical component of the earth field.

Fig. 6), within the ac amplitude independent transition width. We note that this negative curvature of $H_p(T)$ [or $H_{c1}(T)$] is recognized already at temperatures clearly lower than those where a broadening of the shielding signal is observed, see Fig. 6. Note also that the ac field dependence of the susceptibility due to the geometrical barrier is measured in the

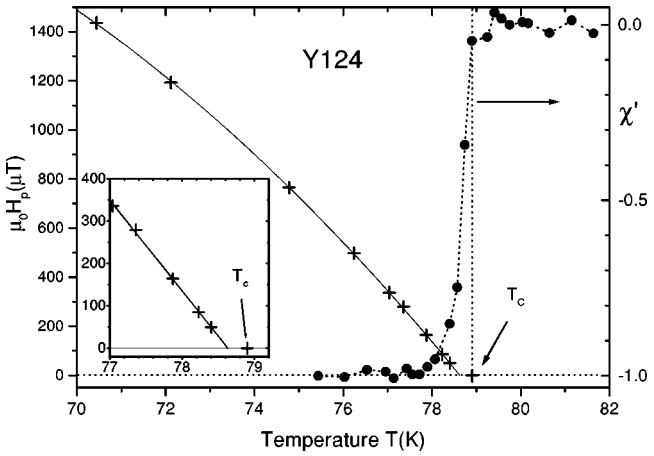

FIG. 6. Penetration field H_p as a function of temperature for the Y124 crystal. For comparison the real component of the susceptibility (measured at $\mu_0 H_0=19$ μT) is also plotted. The inset blows up the region near T_c.

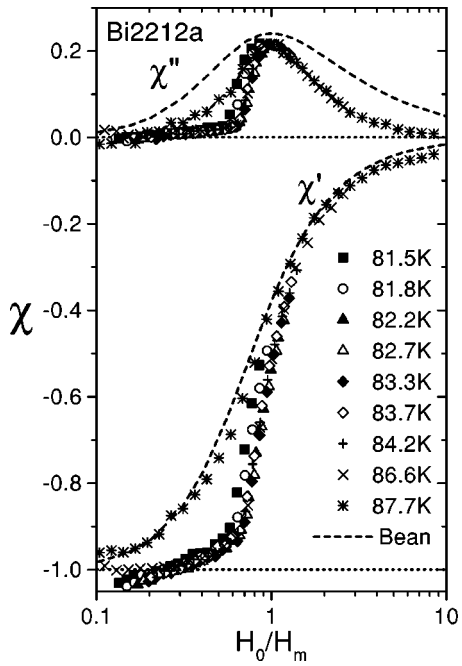

FIG. 7. The two components of the nonlinear ac susceptibility for the Bi2212a crystal (with earth field compensated). The ac field amplitude is normalized by the field of maximum dissipation H_m. At $T=87.7$ K the measured behavior tends to follow the nonlinear Bean-like model (dashed line) calculated as described in Ref. 29.

whole temperature range, including that inside the width of the transition as measured by the real part of the susceptibility at $\mu_0 H_0=19$ μT, see Fig. 6.

Strictly speaking, the breakdown of H_{c1} as observed in Bi2212 in Ref. 5 and in Y123,[2,6] is not observed in Y124 in the measured temperature range, but a temperature dependence with a negative curvature. At temperatures $T>78.6$ K, the ac fields necessary to determine H_p were so small ($<25\mu$T) that no reliable signal could be detected due to the smallness of the crystal.

B. $Bi_2Sr_2CaCu_2O_8$

The nonlinear susceptibility curves with and without normalization for the Bi2212a crystal before and after annealing are shown in Figs. 7 and 8, respectively. At low enough temperatures, the susceptibility of the Bi2212a crystal shows the characteristic response due to the geometrical barrier, as in the Y124 crystal. However, and in contrast to the Y124 crystal, at a temperature $T_{co}\simeq 0.97T_c$ or higher, the nonlinear susceptibility deviates clearly from the predicted behavior of the geometrical barrier model. There is a broadening of the ac field dependence, that tends to the curve obtained from the nonlinear Bean model,[29,17,18,13] see Fig. 7. Therefore, the normalization of the ac field amplitude in Fig. 7 is done by the field at the dissipation maximum H_m and not H_p.

Note that the annealed crystal Bi2212a# shows a decrease of the diamagnetic signal as well as of the dissipation maximum at the highest measured temperatures (see Fig. 8) which lie within the superconducting transition width. If we normalize the susceptibility curves according to $H_0 \rightarrow H_0/H_p$ and $\chi'(H_0\rightarrow 0)\rightarrow -1$ they follow a single curve (see Figs. 7 and 4). However, in contrast to the results for the

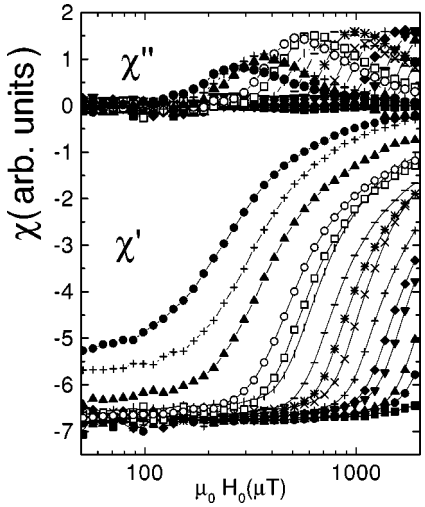

FIG. 8. The same as in Fig. 7 but without normalization, for the annealed crystal Bi2212a#. The temperature of the measurements are (from left to right curves): 89.58, 89.30, 89.13, 88.71, 88.43, 88.10, 87.55, 86.93, 86.14, 85.34, 84.27, 83.03, 81.85, 80.62, and 77.20.

same crystal before annealing (Fig. 7) no broadening of the ac field dependence is observed. The geometrical barrier behavior is measured up to the highest temperature $T=89.58$ K.

We note that the vanishing of the geometrical barrier at T_{co} for the Bi2212a crystal occurs at temperatures when the Meissner signal starts to break down, see also Fig. 9. This

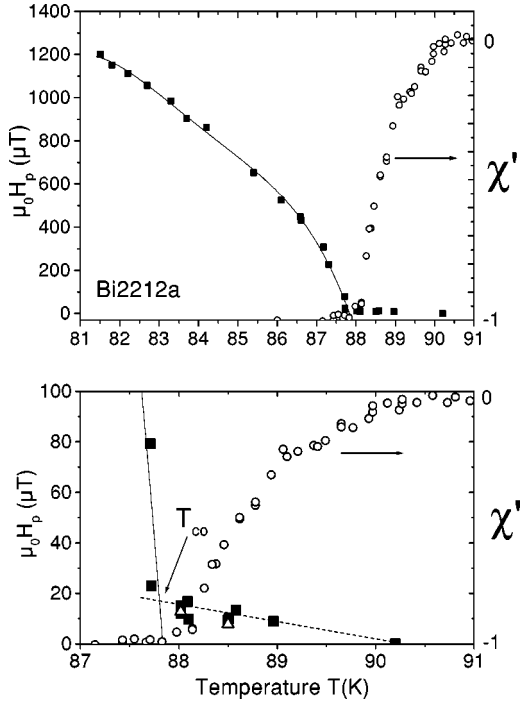

FIG. 9. Penetration field H_p and real component of the susceptibility (right axis) at $\mu_0 H_0=10$ μT, as a function of temperature for the Bi2212a crystal. The lower figure shows the region near T_c on an expanded scale. The data above T_{co} denotes the position of the maximum in the imaginary component of the susceptibility. The data ($\triangle$) have been obtained with a frequency $f=1$ kHz. The lines are only a guide.

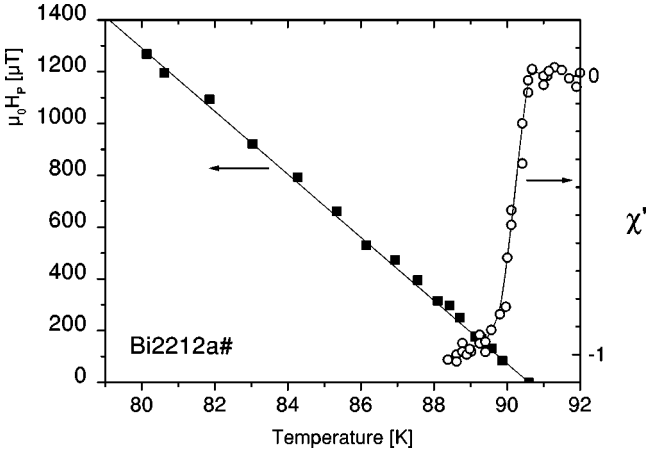

FIG. 10. Penetration field H_p and real component of the susceptibility (right axis) at $\mu_0 H_0=5$ μT, as a function of temperature for the annealed Bi2212a# crystal. The straight line is the fit to the data $H_p(T)=1.1\times10^4[1-(T/90.6)]\mu$T.

loss of the geometrical barrier has been observed in another Bi2212 crystal[11] and is not related to an uncompensated earth field.

From the measurements of the nonlinear susceptibility of the Bi2212 crystals we obtained the penetration field H_p or the lower critical field H_{c1} as for the Y124 crystal. The temperature dependence of $H_p(T)$ for the Bi2212a crystal shows a negative curvature as for the Y124 crystal, see Fig. 6, and vanishes at temperatures just below T_{co} denoted by the arrow in Fig. 9. We stress that this breakdown is not an artifact of the measurements. The abrupt decrease of H_p starts at a temperature $T\simeq85.5$ K, *below* the temperature T_{co} where the real component of the susceptibility deviates from the perfect shielding state. At temperatures $T>T_{co}$ no H_p can be determined from our measurements. In other words $H_p(T>T_{co})\simeq0$. The fields plotted in Fig. 9 above T_{co} are the fields of maximum dissipation H_m. Note that H_m remains finite and tends to vanish approaching T_c, see Fig. 9.

Regarding the influence of inhomogeneities on $H_p(T)$, it is interesting to compare the data of the crystal Bi2212a before and after annealing. The annealed Bi2212a# crystal shows a linear temperature dependence for $H_p(T)$, see Fig. 10, in the whole temperature range. The extrapolation of this dependence to $\mu_0 H_p=0$ μT coincides with the defined critical temperature (see Fig. 1) within experimental error.

The nonlinear susceptibility of the inhomogeneous crystal Bi2212b shows a clear double peak structure as a function of the ac field amplitude at a temperature $T\simeq85.7$ K where the geometrical barrier behavior is lost. Interestingly, the typical geometrical barrier signature due to the existence of H_p is recovered at higher temperatures. At even higher temperatures $T>88$ K this behavior is lost and a Bean-like dependence is observed as for the Bi2212a crystal. In order to study the influence of the sample size to the ac response observed for the inhomogeneous crystal Bi2212b and to see whether the observed behavior is due to some inhomogeneous parts of the crystal rim, we have broken it in the middle and measured one of the remaining pieces. The obtained results are similar to those of the large, original

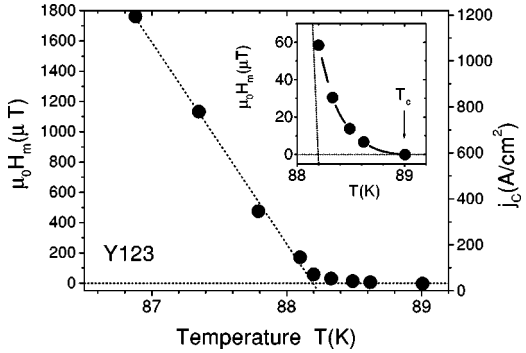

FIG. 11. The amplitude of the ac field, at which the imaginary part of the susceptibility reaches its maximum, as a function of temperature for the Y123 crystal. Following the nonlinear Bean model for transverse geometry, the critical current density can be calculated and is given at the right axis. The inset blows up the region near T_c.

Bi2212b crystal. From all these data it becomes evident that the temperature dependence of H_p is influenced by inhomogeneities.

C. $YBa_2Cu_3O_7$

The Y123 crystal we have measured did not show the same behavior of the nonlinear susceptibility observed in the other crystals. For this crystal we have found no clear sign for geometrical barrier pinning. The ac dependence of the nonlinear susceptibility follows the nonlinear Bean model for bulk pinning. It is perhaps not a surprising result, since it is known that the Y123 superconductor shows larger pinning than the other two HTS's, therefore the weak bulk pinning requirement for the dominance of the geometrical barrier is not fulfilled. Certainly, we cannot rule out that other Y123 crystals, specially produced or treated to lower the bulk pinning, may show the influence of the geometrical barrier. Further studies on other Y123 crystals are necessary to clarify this issue.

It is interesting to analyze the T dependence of H_m for the Y123 crystal. Figure 11 shows the temperature dependence of H_m obtained from the maximum of the imaginary part of the nonlinear susceptibility. For the Y123 crystal we find $H_m(T)$ with a positive curvature. It tends to decrease linearly with temperature up to $T \simeq 0.991 T_c$. At higher temperatures H_m changes its slope and tends to vanish approaching T_c, see inset in Fig. 11.

The observed dependence of $H_m(T)$ is given by the critical current density $j_c(T)$. According to the nonlinear Bean model and for a strip $H_m = 0.78 d j_c$ where d is the thickness of the sample.[13,17,18,29] The values of j_c are given in the right y axis of Fig. 11. The obtained critical current density is much smaller than in Y123 thin films[29] and shows a different temperature dependence. It is interesting to note that j_c does not vanish at $T < T_c$, even at a field of 5 μT, see inset in Fig. 11. Obviously, the absence of the characteristic ac field dependence given by the geometrical barrier prevents the determination of H_{c1} for the Y123 crystal with our method.

IV. DISCUSSION

A clear distinction between the nonlinear response obtained from the geometrical barrier and that from the Bean-Livingston surface barrier is difficult by measuring global or even local nonlinear susceptibility or magnetization. A possible way to study and differentiate the contributions of these two different barrier mechanisms is by changing the shape of the crystals, see Ref. 33. In that work it is shown that in platelet samples with weak bulk pinning and in transverse geometry, the geometrical barrier appears to be the dominant at high temperatures.

One may still ask if the measured response in our crystals shows some evidence for thermally activated relaxation at the low fields of our measurements. For fields below 10 Oe and by changing the frequency of the ac field from 30 Hz to 1 kHz, the signals of the nonannealed crystal Bi2212a show a shift in the position of the maximum of $\chi''(H_0)$ of less than 0.5 K, indicating an activation energy larger than 3 eV. This result cannot be understood within the geometrical barrier model since this leads to a very small probability for thermally activated hopping of vortices. We note, however, that this weak frequency dependence is completely absent in the annealed crystal. It is therefore clear that inhomogeneities influences the frequency dependence of the ac response near T_c.

Taking into account all this evidence and the typical behavior of the nonlinear susceptibility, see Figs. 4, 7, and 8, we argue that the geometrical barrier is the main mechanism for the irreversible behavior in Y124 and Bi2212 crystals at the temperatures and fields of our measurements.

A detailed theory of $H_{c1}(T)$ near T_c, taking into account the influence of self fluctuations of the order parameter, is given by Blatter *et al.*[9] As discussed in Ref. 9, thermal fluctuations shift the transition temperature T_c to lower temperatures. Depending on the anisotropy of the superconductor, this shift can be of the order of 3 K for Bi2212 HTS. Moreover, thermal fluctuations change the curvature of $H_{c1}(T)$ from zero to negative.[9] For the less anisotropic crystals such as Y123 a parallel shift of the $H_{c1}(T)$ without a downward bending is expected from this theory. Taking into account only the results of the Bi2212a and Y124 crystals these theoretical predictions[9] appear to be in good agreement with our observations: the larger the anisotropy, the larger the expected shift to lower temperatures of the lower critical field. The previously published results in the literature indicate also an anomalous temperature dependence for $H_{c1}(T)$ in highly anisotropic high-T_c superconductors. However, we show clearly that the temperature dependence of H_{c1} [the breakdown of $H_{c1}(T)$ near T_c as well as its negative curvature], extracted from $H_p(T)$, is sensitive to the homogeneity of the crystal and it cannot be taken as an intrinsic property.

V. CONCLUSION

In conclusion, we have measured the ac field amplitude dependence of the global susceptibility of different HTS crystals near T_c. For the weak pinning HTS crystals, the ac field amplitude dependence follows the predicted behavior due to the geometrical barrier mechanism. Measuring the

penetration field H_p we have shown that the lower critical field for nonannealed Bi2212 and Y124 crystals shows an anomalous dependence near T_c, vanishing at $T_{co} \sim T_c - 2$ K and $\sim T_c - 0.3$ K, respectively. This ''collapse'' of H_p occurs just at the low-temperature onset of the zero-field superconducting transition and indicates that these effects are not an intrinsic property of the HTS crystals. The measurements on three Bi-based crystals show that the temperature dependence of $H_{c1}(T)$ depends on the sample quality. In particular, the breakdown of $H_{c1}(T)$ as well as the negative curvature is absent for the annealed Bi2212a crystal. For our untwinned Y123 crystal, even very near T_c, bulk pinning overwhelms the geometrical barrier effect.

Our measurements with and without compensation of the earth field show clearly the importance of its shielding for the investigation of the superconducting properties near T_c.

ACKNOWLEDGMENTS

This work was supported by the German-Israeli-Foundation for Scientific Research and Development under Grant No. G-303-114.07/93, the Israel Ministry of Science, the Grant-in-Aid for Scientific Research from the Ministry of Education, Science and Culture, Japan, and by the National Science Foundation under Grant No. DMR-91-20000. F.M. was supported by the Deutsche Forschungsgemeinschaft under Grant No. DFG Br1088/3-3. We thank W. Sadowski for providing us with the Y123 crystal, J. Eisenmenger and P. Leiderer for performing the magneto-optical characterizations, and E. H. Brandt for making available the preprint of his article prior to publication and useful discussions. We thank Marcin Konczykowski for providing us with his unpublished result on the suppression of the breakdown of $H_{c1}(T)$ after annealing the HTS crystals.

*Also at the Institute of Low Temperature and Structure Research, Polish Academy of Sciences, P.O. Box 937, 50-950 Wroclaw, Poland.

[1] Y. Yeshurun, A.P. Malozemoff, F. Holtzberg, and T.R. Dinger, Phys. Rev. B **38**, 11 828 (1988).
[2] H. Safar, H. Pastoriza, F. de la Cruz, D.J. Bishop, L.F. Schneemeyer, and J.V. Waszczat, Phys. Rev. B **43**, 13 610 (1991).
[3] M. Konczykowski, L.I. Burlachkov, Y. Yeshurun, and F. Holtzberg, Phys. Rev. B **43**, 13 707 (1991).
[4] L. Burlachkov, M. Konczykowski, Y. Yeshurun, and F. Holtzberg, J. Appl. Phys. **70**, 5759 (1991).
[5] D.A. Brawner, A Schilling, H. Ott, R. Haug, K. Ploog, and K. von Klitzing, Phys. Rev. Lett. **71**, 785 (1993).
[6] H. Pastoriza, H. Safar, E.F. Righi, and F. de la Cruz, Physica B **194-196**, 2237 (1994).
[7] R. Liang, P. Dosenjh, D. Bonn, W. Hardy, and A. Berlinsky, Phys. Rev. B **50**, 4212 (1994).
[8] L. Bulaevskii, M. Ledvij, and V. Kogan, Phys. Rev. Lett. **68**, 3773 (1992).
[9] G. Blatter, B. Ivlev, and H. Nordborg, Phys. Rev. B **48**, 10 448 (1993).
[10] N. Morozov, E. Zeldov, D. Majer, and B. Khaykovich, Phys. Rev. Lett. **76**, 138 (1996).
[11] M. Wurlitzer, F. Mrowka, P. Esquinazi, K. Rogacki, B. Dabrowski, E. Zeldov, T. Tamegai, and S. Ooi, Z. Phys. B **101**, 561 (1996).
[12] See, for example, E.H. Brandt, Rep. Prog. Phys. **58**, 1465 (1995).
[13] E.H. Brandt, Phys. Rev. B **49**, 9024 (1994).
[14] E.H. Brandt, Phys. Rev. B **50**, 4034 (1994).
[15] P.N. Mikheenko and Yu.E. Kuzovlev, Physica C **204**, 229 (1993).
[16] J. Zhu, J. Mester, J. Lockhart, and J. Turneaure, Physica C **212**, 216 (1993).
[17] E.H. Brandt, M. Indenbom, and A. Forkl, Europhys. Lett. **22**, 735 (1993).
[18] E.H. Brandt and M. Indenbom, Phys. Rev. B **48**, 12 893 (1993).
[19] E. Zeldov, J.R. Clem, M. McElfresh, and M. Darwin, Phys. Rev. B **49**, 9802 (1994).
[20] J. Gilchrist, Physica C **219**, 67 (1994).
[21] J. Gilchrist and M. Konczykowski, Physica C **212**, 43 (1993).
[22] E.H. Brandt, Phys. Rev. Lett. **74**, 3025 (1995).
[23] E. Zeldov, A. Larkin, V. Geshkenbein, M. Konczykowski, D. Majer, B. Khaykovich, V. Vinokur, and H. Shtrikman, Phys. Rev. Lett. **73**, 1428 (1994).
[24] M. Benkraouda and J.R. Clem, Phys. Rev. B **53**, 5716 (1996).
[25] T.B. Doyle and R. Labusch, J. Low Temp. Phys. **105**, 1207 (1996); T.B. Doyle, R. Labusch, and R.A. Doyle, Physica C **290**, 148 (1997).
[26] E. Zeldov, A. Larkin, M. Konczykowski, B. Khaykovich, D. Majer, V. Geshkenbein, and V. Vinokur, Physica C **235-240**, 2761 (1994).
[27] E. Zeldov, D. Majer, M. Konczykowski, A. Larkin, V. Vinokur, V. Geshkenbein, N. Chikumoto, and H. Shtrikman, Europhys. Lett. **30**, 367 (1995).
[28] D. Majer, E. Zeldov, and M. Konczykowski, Phys. Rev. Lett. **75**, 1166 (1995).
[29] M. Wurlitzer, M. Lorenz, K. Zimmer, and P. Esquinazi, Phys. Rev. B **55**, 11 816 (1997).
[30] F. Mrowka, M. Wurlitzer, P. Esquinazi, M. Lorentz, K. Zimmer, and E.H. Brandt, Appl. Phys. Lett. **70**, 898 (1997).
[31] C.P. Bean, Rev. Mod. Phys. **36**, 31 (1964).
[32] E. H. Brandt, Phys. Rev. B **59**, 3369 (1999).
[33] N. Morozov, E. Zeldov, M. Konczykowski, and R. Doyle, Physica C **291**, 113 (1997).
[34] R. Khasamov, Yu. Talamov, W. Assmus, and G. Teiltel'baum, Phys. Rev. B **54**, 13 339 (1996).